

# $\Lambda\bar{\Lambda}-\Sigma\bar{\Sigma}$ channel coupling and quasinuclear level of the hyperon-antihyperon system

R. T. Tyapaev

Moscow Engineering-Physics Institute

I. S. Shapiro

P. N. Lebedev Physics Institute, USSR Academy of Sciences

(Submitted 20 June 1983)

Zh. Eksp. Teor. Fiz. **86**, 39–46 (January 1984)

The partial amplitudes for elastic-scattering and for  $\Sigma\bar{\Sigma} \rightarrow \Lambda\bar{\Lambda}$  transitions are calculated for  $\Lambda$  and  $\bar{\Lambda}$  total kinetic energies in the range from 0 to 500 MeV. The level spectrum for the quasinuclear system  $\Lambda\bar{\Lambda}-\Sigma\bar{\Sigma}$  is found. It is shown that the coupling to the closed  $\Sigma\bar{\Sigma}$  channel decreases appreciably the width of the  $\Lambda\bar{\Lambda}$  resonances. The states in the  $\Sigma\bar{\Sigma}$  channel are manifest as anomalously narrow above-barrier resonances. It is found that the partial cross sections for elastic  $\Lambda\bar{\Lambda}$  scattering in the vicinity of resonances close to the  $\Sigma\bar{\Sigma}$  threshold can have a shape that differs significantly from the Breit-Wigner shape. The physical cause of the phenomenon is investigated. The calculations are performed within the framework of a realistic scheme with one-boson exchange potentials.

## 1. INTRODUCTION

It is known that a storage ring for slow antiprotons (see Ref. 1) affords excellent opportunities for the search and investigation of narrow states of baryon-antibaryon ( $B\bar{B}$ ) systems. This has made it necessary to solve a number of hitherto little investigated problems in the theory of quasinuclear baryonium. These include, in particular, the problem of the coupling of various  $B\bar{B}$  channels. In the quasinuclear approach, the interaction between  $B$  and  $\bar{B}$  is described via the one-boson-exchange (OBE) potentials. Exchange of identical bosons leads to diagonal interaction between  $B$  and  $\bar{B}$ , as well as to transitions between different  $B\bar{B}$  channels. A consistent calculation of the spectrum of quasinuclear baryonium calls therefore for a multichannel approach. So far, however, principal attention was paid to interaction within any one of the  $B\bar{B}$  channels (see Refs. 2 and 3). Only one paper<sup>4</sup> deals with the  $N\bar{N}$  resonance induced by the bound  $\Sigma\bar{\Sigma}$  state on account of  $\Sigma\bar{\Sigma} \rightarrow N\bar{N}$  transitions.

Our purpose is to ascertain the changes that the coupling of the  $\Lambda\bar{\Lambda}$  and  $\Sigma\bar{\Sigma}$  channels produce in the spectrum of the quasinuclear levels of a hyperon-antihyperon system and in the observable amplitudes and cross sections. Some of the investigation results of greatest importance for the experimental search were published earlier.<sup>5</sup> Here we study in greater detail the energy dependence of the cross sections in the region of the resonances, various methods of regularizing the potentials, as well as partial waves not considered in Ref. 5.

The plan of the article is the following. Section 2 contains a description of the potentials employed and a scheme for calculating the elements of the matrix of the reactions. In Sec. 3 is given the obtained level spectrum of the quasinuclear  $\Lambda\bar{\Lambda}-\Sigma\bar{\Sigma}$  system, and the change of the level widths on account of possible transitions between the indicated pairs is investigated. Section 4 is devoted to the behavior of various cross sections in the vicinity of the resonances. The final Sec. 5 formulates briefly the principal results of the work.

## 2. EMPLOYED POTENTIALS AND CALCULATION SCHEME

We consider two coupled two-particle channels,  $\Lambda\bar{\Lambda}$  and  $\Sigma\bar{\Sigma}$  (with isospin  $I=0$ ).<sup>1)</sup> The annihilation processes that take place at distances  $r \lesssim m^{-1}$  ( $m$  is the baryon mass)<sup>2)</sup> are not taken into account here. As shown earlier (see Refs. 2 and 6 and the bibliographies there), the basic properties of baryonium are determined principally by nuclear interaction. On the other hand, the annihilation widths of the levels should be small (1–100 MeV, depending on the orbital momentum  $L$ ), despite the high annihilation intensity.

We are interested in a region of energies close to the thresholds of the considered channels, viz.,  $\Lambda\bar{\Lambda}$  (2231 MeV) and  $\Sigma\bar{\Sigma}$  (2386 MeV). We can therefore use the nonrelativistic potential approach. The interactions between  $\Lambda$  and  $\bar{\Lambda}$  or  $\Sigma$  and  $\bar{\Sigma}$  and the transitions  $\Sigma\bar{\Sigma} \rightarrow \Lambda\bar{\Lambda}$  are described by realistic OBE potentials obtained by  $G$ -transformation from the corresponding  $Y\bar{Y}$  potentials ( $Y$  is a hyperon), given in Ref. 7. To simplify the calculation, we disregarded the tensor forces that lead to mixing of triplet states with  $L=J+1$  and  $L=J-1$  ( $J$  is the total angular momentum of the system). A study of the  $N\bar{N}$  system has shown that the tensor forces are of secondary significance in the determination of the qualitative laws. The spin-orbit interaction in the OBE model is singular at short distances ( $\sim r^{-3}$ ). It was regularized by using the cutoff

$$V_{ij}(r < r_c) = 0.$$

Here  $i$  and  $j$  take on the values 1 ( $\Lambda\bar{\Lambda}$  channel) and 2 ( $\Sigma\bar{\Sigma}$  channel). The cutoff radius 0.64 fm was chosen from the condition  $V_{ij}(r_c) \lesssim m$ . To check on the stability of the basic results to variation of the potentials at short distances, the calculations were performed also with a second cutoff method:

$$V_{ij}(r < r_c) = V_{ij}(r_c).$$

To calculate the  $K$  matrix of the reactions we used the phase-function method,<sup>8</sup> which leads to the equation

$$K'(r) = -[Y(r) + K(r)Z(r)]W(r)[Y(r) + Z(r)K(r)] \quad (1)$$

with boundary condition  $K(0) = 0$ . Here  $K(r)$  is the matrix of the reactions for the potential

$$V_{ij}(r') = V_{ij}(r')\theta(r-r'), \quad W_{ij}(r) = (m_i m_j)^{-1/2} V_{ij}(r),$$

$m_i$  is the mass of the particles in the channel  $i$ ,

$$Y_{ij}(r) = k_i^{-1/2} j_L(k_i r) \delta_{ij}, \quad Z_{ij}(r) = -k_i^{-1/2} n_L(k_i r) \delta_{ij}$$

for open channels,

$$Y_{jj}(r) = (-i)^{L+1} (2|k_j|)^{-1/2} [j_L(i|k_j|r) - i n_L(i|k_j|r)],$$

$$Z_{jj}(r) = i^{L+1} (2|k_j|)^{-1/2} [j_L(i|k_j|r) + i n_L(i|k_j|r)]$$

for closed channels,  $k_j = [m_j(E - 2m_j)]^{1/2}$ , and  $E$  is the total energy.

In the considered case of two coupled channels, the matrix equation (1) reduces to a system of three nonlinear first-order equations for the independent elements of the matrix  $K(r)$ . This system was solved numerically by the scheme described in Ref. 9.

### 3. ARGAND DIAGRAMS AND SPECTRUM OF QUASINUCLEAR LEVELS

Having calculated the reaction matrix  $K$ , it is easy to obtain the  $S$  matrix

$$S(E) = (1 - iK)^{-1} (1 + iK).$$

To determine the masses and widths of the resonances, we plotted Argand diagrams that describe the behavior of the dimensionless quantities

$$k_{1f11} = (S_{11} - 1)/2i, \quad k_{2f22} = (S_{22} - 1)/2i$$

on the complex plane. Here  $f$  are the elastic-scattering partial amplitudes. On these diagrams the resonances appear in the form of rapid counterclockwise motion of the point with increasing energy. By way of example, Fig. 1 shows the behavior of the  ${}^3P_0$  amplitudes obtained with the first cutoff method.

The parameters of the resonances were obtained on the basis of the energy dependence of the  $S$ -matrix elements

$$S_{ij}(E) = \exp(2i\delta_j^b) [1 - i\Gamma_j / (E - m_R + i\Gamma/2)]. \quad (2)$$

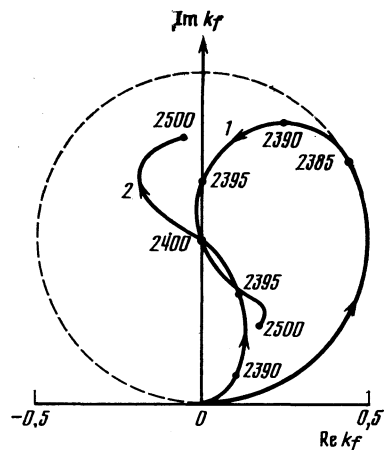


FIG. 1. Argand diagram for  ${}^3P_0$  amplitudes of the  $\Lambda\bar{\Lambda}$  (curve 1) and  $\Sigma\bar{\Sigma}$  (curve 2) elastic scattering for the first cutoff method. The numbers at the points are the total energies (MeV). The unit circle is shown dashed.

Here  $\delta_j^b = \delta_j^b(E)$  is the background phase (a slowly varying function of the energy). The resonance mass  $m_R$  was taken to be the energy at which the  $S$  matrix changes most rapidly. The total width  $\Gamma = \Gamma_1 + \Gamma_2$  and the partial width  $\Gamma_1$  in the  $\Lambda\bar{\Lambda}$  channel were calculated from the equations

$$\Gamma = 4(|S_{11}'| + |S_{22}'|)^{-1},$$

$$\Gamma_1 = \Gamma |S_{11}'| (|S_{11}'| + |S_{22}'|)^{-1},$$

where all the derivatives were taken at the point  $E = m_R$ .

Since we are solving a scattering problem, such a method does not make it possible to find levels below the  $\Lambda\bar{\Lambda}$  threshold. We can, however, indicate the energies of these states without taking the  $\Sigma\bar{\Sigma} \rightleftharpoons \Lambda\bar{\Lambda}$  transitions into account. To this end we introduce a fictitious channel of light particles that is weakly coupled to the  $\Lambda\bar{\Lambda}$  or  $\Sigma\bar{\Sigma}$  channel. In the fictitious channel the  $\Lambda\bar{\Lambda}$  or  $\Sigma\bar{\Sigma}$  level will appear as a very narrow resonance. Provided that there is no lower-lying bound state with the same quantum numbers, the energy of such a level can only be decreased<sup>3)</sup> on account of the virtual  $\Lambda\bar{\Lambda} \rightleftharpoons \Sigma\bar{\Sigma}$  transitions. If, however, two levels exist below the  $\Lambda\bar{\Lambda}$  threshold, the mass of the heavier of them will increase.

All the  $\Lambda\bar{\Lambda}$ - $\Sigma\bar{\Sigma}$  system levels obtained in this manner are listed in the table, which gives also their parameters obtained without allowance for the possible  $\Lambda\bar{\Lambda} \rightleftharpoons \Sigma\bar{\Sigma}$  transitions. It can be seen from the table that the coupling to the closed  $\Sigma\bar{\Sigma}$  channel decreases noticeably the widths of the  $\Lambda\bar{\Lambda}$  resonances. An example that shows this most pronouncedly is the resonance  ${}^3F_3$  (2250), whose width decreases by four orders. The physical cause of this phenomenon is that the additional attraction due to the virtual transitions  $\Lambda\bar{\Lambda} \rightleftharpoons \Sigma\bar{\Sigma}$  leads to a decrease of the excitation energy (from 320 to 20 MeV relative to the  $\Lambda\bar{\Lambda}$  threshold in the case of the aforementioned resonance  ${}^3F_3$ ). The penetrability of the centrifugal barrier is then increased and the width of the resonance decreased.

Another mechanism that generates narrow states in a light-particle channel was indicated earlier also in Ref. 4. The levels of the  $\Sigma\bar{\Sigma}$  system will manifest themselves as anomalously narrow highly excited  $\Lambda\bar{\Lambda}$  resonances. In our case the states of this type are the resonances  ${}^3S_1$  (2327),  ${}^1S_0$  (2357),  ${}^3P_0$  (2396),  ${}^3P_1$  (2394),  ${}^3P_2$  (2399),  ${}^1P_1$  (2403) and  ${}^3P_0$  (2390),  ${}^3P_1$  (2388),  ${}^3P_2$  (2357),  ${}^1P_1$  (2384). Thus, the width of the  ${}^3P_0$  (2390) resonance is only 17 MeV (see the table), although its excitation energy  $E_R = 160$  MeV greatly exceeds the height  $V_c = 15$  MeV of the centrifugal barrier. For the above-barrier resonances, in addition, it would be natural to expect a width  $\Gamma \gtrsim 200$  MeV, as for the  ${}^3D_3$  (2351) resonance, which has  $E_R = 120$  MeV,  $V_c = 85$  MeV, and  $\Gamma = 220$  MeV.

We note that the sufficiently strong interaction that relates the channels  $\Lambda\bar{\Lambda}$  and  $\Sigma\bar{\Sigma}$  can lead to the appearance of new levels. Such is the situation with the resonance  ${}^1S_0$  (2385) and with the coupled states  ${}^3P_0$  ( $\leq 2230$ ) and  ${}^3P_1$  ( $\leq 2230$ ), which are quite close to the  $\Lambda\bar{\Lambda}$  threshold (see the table). The existence of the last two levels is indicated by the appreciable increase of the  $\Lambda\bar{\Lambda}$  elastic-scattering cross section at low kinetic energies.

It can be seen from the table that the total number of the levels and their sequence depend little on the method used to

TABLE I. Spectrum of isoscalar levels of the quasinuclear system  $\Lambda\bar{\Lambda} + \Sigma\bar{\Sigma}$  with allowance ( $\Lambda\bar{\Lambda} + \Sigma\bar{\Sigma}$ ) and without allowance ( $\Lambda\bar{\Lambda}, \Sigma\bar{\Sigma}$ ) of the possible transitions between the indicated pairs ( $2m_{\Lambda} = 2331$  MeV,  $2m_{\Sigma} = 2386$  MeV)

$2S+1L_J$	Mass, MeV			$\Gamma = \Gamma_{\Lambda\bar{\Lambda}} + \Gamma_{\Sigma\bar{\Sigma}}$ , MeV			$\Gamma_{\Lambda\bar{\Lambda}}/\Gamma$
	$\Lambda\bar{\Lambda} + \Sigma\bar{\Sigma}$	$\Lambda\bar{\Lambda}$	$\Sigma\bar{\Sigma}$	$\Lambda\bar{\Lambda} + \Sigma\bar{\Sigma}$	$\Lambda\bar{\Lambda}$	$\Sigma\bar{\Sigma}$	$\Lambda\bar{\Lambda} + \Sigma\bar{\Sigma}$
With cutoff $V_{ij}(r < r_c) = 0$							
${}^3S_1$	$\sphericalangle$ 2146 2327	2146	2323	5,5			—
${}^1S_0$	$\sphericalangle$ 2193 2357	2193	2331	32			1
${}^3P_0$	$\sphericalangle$ 2210 2396	2210	2391	34		6	0,46
${}^3P_1$	$\sphericalangle$ 2225 2394	2225	2392	27,5		6,5	0,46
${}^3P_2$	2241 2399	2242	2398	12 23	15	19	1 0,19
${}^1P_1$	2247 2403	2251	2402	29 50	48	27	1 0,18
${}^3D_1$	2280	2328		15	105		1
${}^3D_2$	2330	2340		100	195		1
${}^3F_2$	2450	2550		76	440		0,96
${}^3F_3$	2540	2560		250	700		0,73
With cutoff $V_{ij}(r < r_c) = V_{ij}(r_c)$							
${}^3S_1$	$\sphericalangle$ 1800 $\sphericalangle$ 2065	1800	2065				
${}^1S_0$	$\sphericalangle$ 2030 $\sphericalangle$ 2230 2385	2030	2103				1
${}^3P_0$	$\sphericalangle$ 1860 2390	1860	2250	17			0,54
${}^3P_1$	$\sphericalangle$ 2230 $\sphericalangle$ 1970 2388	1970	2285	23			0,74
${}^3P_2$	$\sphericalangle$ 2230 $\sphericalangle$ 2150 2357	2150	2338	26			1
${}^1P_1$	$\sphericalangle$ 2213 2384	2213	2326	105			1
${}^3D_1$	$\sphericalangle$ 2100	2100	2456			52	
${}^3D_2$	$\sphericalangle$ 2230	2262	2490		5	90	
${}^3D_3$	2349	2351		127	219		1
${}^1D_2$	2360	2361		240	250		1
${}^3F_2$	—	2405			38		
${}^3F_3$	2250	2550		0,025	290		1

cut off the potentials at short distances, although the level energies can be considerably altered in this case.

#### 4. ENERGY DEPENDENCES OF THE CROSS SECTIONS NEAR THE RESONANCES

In this section we consider the behavior of the partial and total cross sections for  $\Lambda\bar{\Lambda}$  and  $\Sigma\bar{\Sigma}$  elastic scattering and for the reaction  $\Sigma\bar{\Sigma} \rightarrow \Lambda\bar{\Lambda}$  in the vicinities of the resonances obtained in Sec. 3. The partial cross sections  $\sigma_{11}(\Lambda\bar{\Lambda} \rightarrow \Lambda\bar{\Lambda})$ ,  $\sigma_{22}(\Sigma\bar{\Sigma} \rightarrow \Sigma\bar{\Sigma})$  and  $\sigma_{12}(\Sigma\bar{\Sigma} \rightarrow \Lambda\bar{\Lambda})$  are connected with the  $S$ -matrix elements by the known relations:

$$\sigma_{ij}(E) = \pi k_j^{-2} (2J+1) |\delta_{ij} - S_{ij}|^2.$$

The most important for exploratory experiments is the fact that near certain resonances the excitation curves  $\sigma_{22}(E)$ ,  $\sigma_{12}(E)$ , and  $\sigma_{11}(E)$  can take substantially different forms. Thus, in the vicinity of the levels  ${}^3S_1$  (2327),  ${}^1S_0$  (2357),  ${}^3P_0$  (2396),  ${}^3P_1$  (2394),  ${}^3P_2$  (2399),  ${}^1P_1$  (2403) (see the table) a minimum is observed in the cross section  $\sigma_{11}$  (see Fig. 2a for the  ${}^3P_0$  cross sections). In the second cutoff method the

cross section  $\sigma_{11}$  near the resonances  ${}^3P_0$  (2390) and  ${}^3P_1$  (2388) show in succession a maximum and a minimum (see the  ${}^3P_0$  cross sections in Fig. 2b). At the same time the cross sections  $\sigma_{22}$  and  $\sigma_{12}$  show the usual peaks near the resonances in all cases. The strong difference between the forms of the cross section  $\sigma_{11}$  in the vicinity of the indicated highly excited resonances, on the one hand, and the Breit-Wigner maximum, on the other, is explained by interference with the  $\Lambda\bar{\Lambda}$  "eigenlevel" that is close enough to the threshold. Indeed, in each of the listed cases there exists one more lower-lying level with the same quantum numbers. Therefore the background phase  $\delta_1^b$  in Eq. (2) may be not small near the heavy resonance. Its value is determined by the relation between the energies of the two states relative to the  $\Lambda\bar{\Lambda}$  threshold: the closer the lighter level to the threshold, the faster the change of the background phase it produces. Thus, in the first cutoff method there exist levels  ${}^3P_0$  and  ${}^3P_1$  with binding energy  $E_B = 10 - 20$  MeV in the  $\Lambda\bar{\Lambda}$  system. With increasing kinetic energy  $E_1$  of the  $\Lambda\bar{\Lambda}$  pair, from  $E_1 = 0$  to  $E_1 \approx 160$  MeV, the phase  $\delta_1^b(E_1)$  decreases from

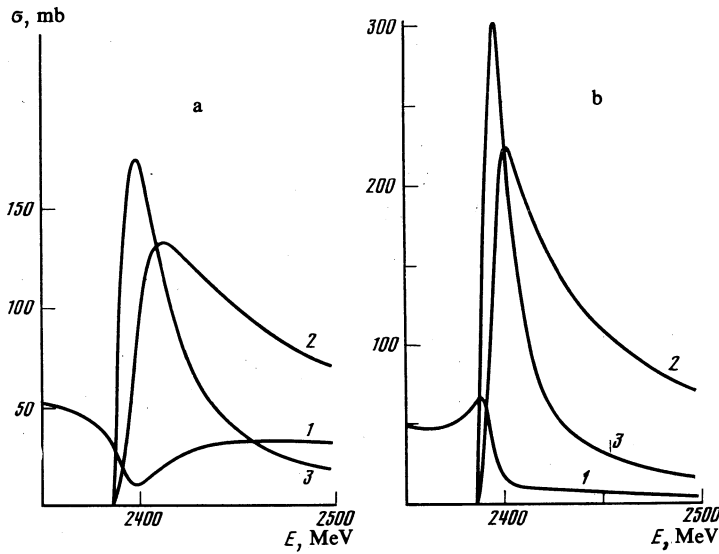


FIG. 2. Energy dependence of the partial cross sections for  $\Lambda\bar{\Lambda}$  (curves 1) and  $\Sigma\bar{\Sigma}$  (curves 2) elastic scattering and for the reaction  $\Sigma\bar{\Sigma} \rightarrow \Lambda\bar{\Lambda}$  (curves 3) near the following resonances: a)  ${}^3P_0$  (2396) with cutoff  $V_{ij}(r < r_c) = 0$ , b)  ${}^3P_0$  (2390) with cutoff  $V_{ij}(r < r_c) = V_{ij}(r_c)$ .

$\pi(\delta_1^b(0) = \pi n$ , where  $n$  is the number of bound states below the  $\Lambda\bar{\Lambda}$  threshold) to  $\pi/2$ . The cross section  $\sigma_{11}$  has therefore a minimum<sup>4)</sup> near the resonances  ${}^3P_0$  (2396) and  ${}^3P_1$  (2394). In the second cutoff method the binding energy of the levels with these quantum numbers is much smaller ( $E_B \lesssim 5$  Mev). Therefore the phase  $\delta_1^b$  has time to change from  $\delta_1^b(0) = 2\pi$  (in this case there exist two levels below the  $\Lambda\bar{\Lambda}$  threshold) to  $\delta_1^b(160 \text{ MeV}) \approx 5\pi/4$ . The cross section  $\sigma_{11}$  in the vicinity of the resonances  ${}^3P_0$  (2390) and  ${}^3P_1$  (2388) passes then first through a maximum ( $\delta(E_{\max}) \approx 3\pi/2$ ) and then through a minimum ( $\delta(E_{\min}) \approx 2\pi$ ). The binding energy of the levels  ${}^3P_2$  and  ${}^1P_1$  is about 100 MeV. Accordingly, the phase  $\delta_1^b$  decreases from  $\delta_1^b(0) = \pi$  only to  $\delta_1^b(140 \text{ MeV}) \approx 3\pi/4$ . Therefore the cross section  $\sigma_{11}$  near the levels  ${}^3P_2$  (2357) and  ${}^1P_1$  (2384) first reaches a minimum ( $\delta(E_{\min}) \approx \pi$ ), and then a maximum ( $\delta(E_{\max}) \approx 3\pi/2$ ).

Figure 3 shows the total cross section for elastic scattering of  $\Lambda\bar{\Lambda}$  (curve 1) and  $\Sigma\bar{\Sigma}$  (curve 2), and for the reaction

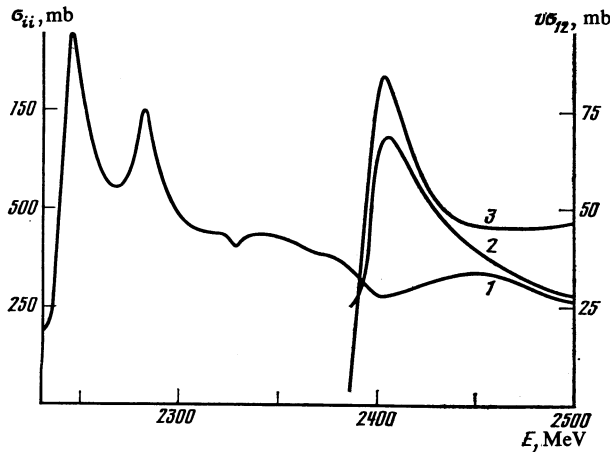


FIG. 3. Energy dependence of the total cross sections for  $\Lambda\bar{\Lambda}$  (curve 1) and  $\Sigma\bar{\Sigma}$  (curve 2) elastic scattering, and values of  $v\sigma$  (curve 3, where  $v$  is the relative velocity of  $\Sigma$  and  $\bar{\Sigma}$ ,  $\sigma$  is the total cross section for the  $\Sigma\bar{\Sigma} \rightarrow \Lambda\bar{\Lambda}$  reaction) in the energy range from the  $\Lambda\bar{\Lambda}$  threshold (2231 MeV) to 2500 MeV.

$\Sigma\bar{\Sigma} \rightarrow \Lambda\bar{\Lambda}$  (curve 3) in the energy range from the  $\Lambda\bar{\Lambda}$  threshold (2231 MeV) to 2500 MeV. The plotted cross sections were obtained with the first cutoff method with account taken of all the partial waves up to  $L = 3$  inclusive. The contribution of the waves with higher orbital momenta is negligibly small in the indicated energy region. The considered energy interval contains 11 resonances (see the left-hand part of the table), which manifest themselves quite distinctly in the corresponding partial cross sections. At the same time, the energy dependences of the total cross sections reveal only four irregularities, at 2245, 2280, 2327, and 2304 MeV. Thus, to observe the hyperon-antihyperon resonances considered in the present paper it may be useful to separate definite partial waves with good statistics and with an energy resolution on the order of 1 MeV. As already noted in Ref. 5, such conditions can be realized with the LEAR setup in experiments on the process  $p\bar{p} \rightarrow \Lambda\bar{\Lambda}$  or  $p\bar{p} \rightarrow \Sigma\bar{\Sigma}$ .

## 5. CONCLUSION

We obtained the following basic results:

1. The width of  $\Lambda\bar{\Lambda}$  resonances is noticeably decreased by the additional attraction due to the coupling with the closed  $\Sigma\bar{\Sigma}$  channel.
2. The  $\Sigma\bar{\Sigma}$  levels manifest themselves in the  $\Lambda\bar{\Lambda}$  channel as anomalously narrow resonances.
3. A sufficiently strong coupling of different  $B\bar{B}$  channels can lead to the appearance of additional quasinuclear levels.
4. The cross section for  $\Lambda\bar{\Lambda}$  elastic scattering in the vicinity of a resonance having a mass close to the  $\Sigma\bar{\Sigma}$  threshold can have a form greatly different from that of the Breit-Wigner peak. The physical cause of this phenomenon lies in the interference with a level that is close enough to the  $\Lambda\bar{\Lambda}$  threshold and has the same quantum numbers.
5. A reliable observation of resonances of quasinuclear type may call for an energy resolution of the order of 1 MeV, with an obligatory separation of definite partial waves and with sufficient statistics.
6. The basic qualitative properties of the quasinuclear

hyperon-antihyperon system depend little on the method used to cut off the potentials at short distances.

The authors thank D. D. Dal'karov and V. E. Markushin for helpful discussions.

<sup>1</sup>The  $\Sigma\bar{\Sigma} \rightarrow \Lambda\bar{\Lambda}$  transitions can take place only from states with  $I = 0$ , since the  $\Lambda$ -hyperon isospin is zero, and the coupling of the  $\Lambda\bar{\Lambda}$  and  $\Sigma\bar{\Sigma}$  channels is due to isospin-conserving nuclear interactions.

<sup>2</sup>Here and elsewhere we use a system of units in which  $\hbar = c = 1$ .

<sup>3</sup>See Ref. 10 concerning the level shifts due to virtual transitions into a closed channel.

<sup>4</sup>The form of the energy dependence of the cross section near the resonance, at various values of the background phase, was considered in detail in Ref. 11.

<sup>1</sup>CERN Courier 22, 365 (1982).

<sup>2</sup>I. S. Shapiro, Phys. Rep. 35C, 129 (1978). Usp. Fiz. Nauk 125, 577 (1978) [Sov. Phys. Usp. 21, 645 (1978)].

<sup>3</sup>C. B. Dover and M. Goldhaber, Phys. Rev. D15, 1997 (1977); W. W. Buck, C. B. Dover, and J. M. Richard, Ann. Phys. (NY) 121, 47 (1979).

<sup>4</sup>L. N. Bogdanova and V. E. Makushin, Yad. Fiz. 32, 512 (1980) [Sov. J. Nucl. Phys. 32, 263 (1980)].

<sup>5</sup>R. T. Tyapaev and I. S. Shapiro, Pis'ma Zh. Eksp. Teor. Fiz. 37, 291 (1983) [JETP Lett. 37, 345 (1983)].

<sup>6</sup>R. T. Tyapaev, Zh. Eksp. Teor. Fiz. 82, 369 (1982) [Sov. Phys. JETP 55, 209 (1982)].

<sup>7</sup>M. M. Nagels, A. Rijken, and J. J. deSwart, Phys. Rev. D20, 1633 (1979).

<sup>8</sup>V. V. Babikov, Metod fazovykh funktsii v kvantovoi mekhanike (Method of Phase Functions in Quantum Mechanics), Nauka, 1976. F. Calogaro, Variable-phase approach to potential scattering, Academic, 1967.

<sup>9</sup>M. P. Faifman, Yad. Fiz. 26, 433 (1977) [Sov. J. Nucl. Phys. 26, 309 (1977)].

<sup>10</sup>B. O. Kerbikov, A. E. Kudryavtsev, V. E. Markushin, and I. S. Shapiro, Pis'ma Zh. Eksp. Teor. Fiz. 26, 505 (1977) [JETP Lett. 26, 368 (1977)].

<sup>11</sup>J. R. Taylor, Scattering Theory, Wiley, 1972.

Translated by J. G. Adashko